Available online at www.sciencedirect.com
ScienceDirect
Journal of Solid State Chemistry 180 (2007) 3479–3484
JOURNAL OF SOLID STATE CHEMISTRY
www.elsevier.com/locate/jssc

Preparation and characterization of a novel hybrid magnetic semiconductor containing rare, one-dimensional mixed-iodide/chloride anion of lead(II)

Le-Qing Fan*, Ji-Huai Wu*, Yun-Fang Huang

Key Laboratory for Functional Materials of Fujian Higher Education, Institute of Materials Physical Chemistry, Huaqiao University, Quanzhou, Fujian 362021, PR China

Received 5 August 2007; received in revised form 6 October 2007; accepted 8 October 2007
Available online 17 October 2007

Abstract

A new hybrid inorganic–organic magnetic semiconductor $[Ni(bipy)_3Pb_2I_{4.84}Cl_{1.16}\cdot DMF]_n$ (bipy = 2,2′-bipyridine) containing novel one-dimensional mixed-halide anion of lead(II) was synthesized by reactions of PbI_2, NaI, $NiCl_2$ and bipy in DMF solution, and structurally characterized by single-crystal X-ray diffraction. It crystallizes in the space group $C2/c$ with $a = 29.260(8)$ Å, $b = 15.602(4)$ Å, $c = 23.695(6)$ Å, $\beta = 126.815(^\circ)$, $Z = 8$, $V = 8660(4)$ Å^3 and consists of a magnetic cation $[Ni(bipy)_3]^{2+}$ in addition to one-dimensional mixed-halide anion, which is built up of face-sharing $[PbX_6]$ octahedra. Of the seven crystallographically independent halide sites in this anion, one and five are occupied by Cl and I, respectively, the remaining one has mixed-iodide and -chloride occupancy. The title yellow compound has an optical bandgap of 2.59 eV, and the variable-temperature magnetic susceptibility measurement indicates paramagnetic behavior.

Keywords: Mixed iodide/chloride anion; Magnetic semiconductor; Crystal structure; Characterization

1. Introduction

The chemistry of the haloplumbates has been studied for several years owing to their significant structural, excitonic, nonlinear optical, semiconducting, and other physical properties [1]. Consequently, numerous complex haloanions of lead have been found to exhibit a great deal of diversity in their structures. Their structural diversity is provided by the flexibility of the Pb^{2+} coordination polyhedron and the nature of halide anions, which can be modulated by the size and H-bonding properties of the cations. The structural diversity is also dependent upon the synthetic conditions employed including reactant concentrations, solvents, reaction temperature, crystallization conditions, etc. [2]. Their anion structures range from isolated anions [2a,3] to infinite chains [4], layered perovskites [5], and three-dimensional polymeric networks [6]. Most structures are characterized by $[PbX_6]$ octahedra with common faces, edges, or vertices. Interestingly, despite the number and diversity of known haloplumbates, mixed halides of lead are comparatively rare [7].

On the other hand, Coronado and Day have pointed out that the combination of magnetic moments with conduction electrons in one compound may give rise to a simple superposition of magnetic and conducting properties if the two compositions are electronically independent or to a mutual influence between these properties if they interact. So the idea is that besides fine-tune the structure of inorganic haloanion, the cation can act as magnetic complex coassembling with the inorganic semiconductor haloplumbate to form a type of magnetic semiconductor [8]. Herein, we wish to report the synthesis and single-crystal X-ray structure of a novel magnetic semiconductor $[Ni(bipy)_3Pb_2I_{4.84}Cl_{1.16}\cdot DMF]_n$ (bipy = 2,2′-bipyridine) which contains one-dimensional mixed-halide anion of lead(II).

*Corresponding authors. Fax: +86 595 22693999.
E-mail addresses: lqfan@hqu.edu.cn (L.-Q. Fan), jhwu@hqu.edu.cn (J.-H. Wu).

0022-4596/$ - see front matter © 2007 Elsevier Inc. All rights reserved.
doi:10.1016/j.jssc.2007.10.010

2. Experimental section

2.1. Materials and methods

All of the reagent-grade reactants were commercially available and employed without further purification. X-ray powder diffraction data were measured on a DMAX2500 diffractometer. Element analyses were performed on Vario EL III element analyzer. Diffuse reflectance spectrum was measured at room temperature with a Perkin-Elmer Lambda35 UV–vis spectrometer equipped with an integrating sphere, and the $BaSO_4$ plate was used as the reference. Thermogravimetric analysis was performed on a Netzsch Sta449C thermoanalyzer under N_2 atmosphere in the range of 40–1000 °C at a heating rate of 10 °C/min. Magnetic studies were performed with a PPMS-9T magnetometer. A diamagnetic correction was estimated from Pascal's constants [9]. The temperature dependence of the magnetic susceptibilities was investigated over the temperature range of 2–300 K under a magnetic field of 5 kOe.

2.2. Synthesis of $[Ni(bipy)_3Pb_2I_{4.84}Cl_{1.16}\cdot DMF]_n$ (1)

PbI_2 (92 mg, 0.2 mmol) and $NaI\cdot 2H_2O$ (9 mg, 0.05 mmol) were dissolved in DMF (10 mL) at room temperature and in air, and then $NiCl_2\cdot 6H_2O$ (24 mg, 0.1 mmol) was added to the solution and stirred for 5 min. Finally bipy (47 mg, 0.3 mmol) was added to the solution and stirred for another 5 min, and a brown-yellow solution was obtained. About 20 mL of i-PrOH was diffused to the resulting solution, 83 mg of yellow crystals were obtained after about 1 week (a yield of 49.7% based on PbI_2). Elemental analysis (dried) (%) calculated for **1**: C, 23.75; H, 1.81; N, 5.87. Found: C, 23.56; H, 1.98; N, 5.99.

2.3. Determination of crystal structure

Suitable single crystal of **1** was selected and mounted on the end of thin glass fiber using epoxy oil. X-ray diffraction measurements were performed on a Rigaku AFC7R diffractometer at room temperature with the aid of Mo$K\alpha$ radiation ($\lambda = 0.71073$ Å). The data were reduced by *CrystalClear* program [10]. The structure was solved by direct methods with the aid of Bruker SHELXL-97 software package of crystallographic software [11]. The difference Fourier map based on these atomic positions yields the non-H atoms. The structure was refined using full-matrix least-squares refinement on F^2 with SHELXL-97 program. The asymmetric unit contains the $[Ni(bipy)_3]^{2+}$ cation, the "Pb_2I_5Cl" inorganic repeat unit, and one DMF molecule. All hydrogen atoms of the cation and DMF molecular could be located in the difference map. For the final refinement, hydrogens were placed in geometrically idealized positions and included as riding atoms. Preliminary refinement of one apical site of halide of inorganic chain as fully occupied resulted in unreasonably large or small displacement ellipsoids when refined as either I or Cl due to statistical I/Cl disorder on this site. The affected atom is I(1) (final label scheme). Site occupation factor for this mixed I/Cl position was refined subject to summing to unity. Positional and displacement parameters were held equal due to the fact that the atoms are too close in space to refine independently. The final refined occupancy ratios are I(1)/Cl(1) 0.687(3)/0.313(3). A fractional occupancy/vacancy model was not considered as this would violate charge neutrality. No unusual problems were observed for other sites of halide atoms. The final refined composition is then "$Pb_2I_{4.84}Cl_{1.16}$". All non-hydrogen atoms were refined anisotropically; hydrogens were calculated and included as riding atoms. The anisotropic refinement converged to $R_1 = 0.0513$, $wR_2 = 0.1520$ for $I > 2\sigma(I)$ data. Some refinement details and crystal data are gathered in Table 1. Selected bond lengths and angles are listed in Table 2.

Table 1
Crystallographic data and structure refinement parameters for compound **1**

	$Ni(C_{10}H_8N_2)_3Pb_2I_{4.84}Cl_{1.16}\cdot C_3H_7NO$
Empirical formula	$C_{33}H_{31}Cl_{1.16}I_{4.84}N_7NiOPb_2$
Formula weight	1670.40
Color and habit	Orange, prism
Crystal size (mm^3)	$0.24\times 0.20\times 0.18$
Crystal system	Monoclinic
Space group	$C2/c$
a (Å)	29.260(8)
b (Å)	15.602(4)
c (Å)	23.695(6)
β (deg)	126.815(4)
V ($Å^3$)	8660(4)
Z	8
T (K)	293(2)
Density, calculated ($g\,cm^{-3}$)	2.562
Absorption coefficient (mm^{-1})	11.747
$F(000)$	6035
λ (Å)	0.71073
h, k, and l range	−37 to 37, −20 to 20, −30 to 22
Reflections measured	32,270
Independent reflections	9741 [R(int) = 0.0268]
Refinement method	Full-matrix least-squares on F^2
Θ range for data collection (deg)	2.53–27.47
Goodness-of-fit on F^2	0.996
Final R indices [$I>2\sigma$ (I)][a]	$R_1 = 0.0513$, $wR_2 = 0.1521$
R indices (all data)[a]	$R_1 = 0.0576$, $wR_2 = 0.1614$
Largest difference peak and hole ($e\,Å^{-3}$)	3.259 and −3.334

[a] $R_1 = \Sigma||F_0|-|F_c||/\Sigma|F_0|$, $wR_2 = [\Sigma w(|F_0^2|-|F_c^2|)^2/\Sigma w(F_0^2)^2]^{1/2}$.

3. Results and discussion

3.1. Synthesis

The formation of the compound **1** was under solution condition at room temperature. Series of experiments using

Table 2
Selected bond lengths (Å) and angles (deg) for compound **1**

Pb(1)–I(1)	2.9479(17)	Pb(3)–Cl(2)#2	2.860(2)
Pb(1)–I(2)	3.3741(12)	Pb(3)–Cl(2)	2.860(2)
Pb(1)–I(2)#1	3.3741(12)	Pb(3)–I(6)#2	3.2386(9)
Pb(1)–I(3)	3.1185(12)	Pb(3)–I(6)	3.2386(9)
Pb(1)–I(3)#1	3.1185(12)	Pb(3)–I(2)	3.3414(9)
Pb(1)–I(4)	3.4058(14)	Pb(3)–I(2)#2	3.3414(9)
Pb(2)–Cl(2)	2.851(3)	Ni(1)–N(6)	2.079(7)
Pb(2)–I(5)	3.0232(9)	Ni(1)–N(4)	2.081(8)
Pb(2)–I(3)	3.2280(11)	Ni(1)–N(2)	2.086(7)
Pb(2)–I(4)	3.2676(9)	Ni(1)–N(1)	2.090(8)
Pb(2)–I(6)	3.2792(10)	Ni(1)–N(5)	2.093(7)
Pb(2)–I(2)	3.4705(9)	Ni(1)–N(3)	2.094(7)
I(1)–Pb(1)–I(3)#1	90.375(19)	Cl(2)#2–Pb(3)–Cl(2)	180.00(5)
I(1)–Pb(1)–I(3)	90.375(19)	Cl(2)#2–Pb(3)–I(6)#2	85.92(6)
I(3)#1–Pb(1)–I(3)	179.25(4)	Cl(2)–Pb(3)–I(6)#2	94.08(6)
I(1)–Pb(1)–I(2)#1	100.179(15)	Cl(2)#2–Pb(3)–I(6)	94.08(6)
I(3)#1–Pb(1)–I(2)#1	85.57(3)	Cl(2)–Pb(3)–I(6)	85.92(6)
I(3)–Pb(1)–I(2)#1	94.29(3)	I(6)#2–Pb(3)–I(6)	180.0
I(1)–Pb(1)–I(2)	100.179(15)	Cl(2)#2–Pb(3)–I(2)	97.29(6)
I(3)#1–Pb(1)–I(2)	94.29(3)	Cl(2)–Pb(3)–I(2)	82.71(6)
I(3)–Pb(1)–I(2)	85.57(2)	I(6)#2–Pb(3)–I(2)	93.63(2)
I(2)#1–Pb(1)–I(2)	159.64(3)	I(6)–Pb(3)–I(2)	86.37(2)
I(1)–Pb(1)–I(4)	180.0	Cl(2)#2–Pb(3)–I(2)#2	82.71(6)
I(3)#1–Pb(1)–I(4)	89.625(19)	Cl(2)–Pb(3)–I(2)#2	97.29(6)
I(3)–Pb(1)–I(4)	89.625(19)	I(6)#2–Pb(3)–I(2)#2	86.37(2)
I(2)#1–Pb(1)–I(4)	79.821(15)	I(6)–Pb(3)–I(2)#2	93.63(2)
I(2)–Pb(1)–I(4)	79.821(15)	I(2)–Pb(3)–I(2)#2	180.0
Cl(2)–Pb(2)–I(5)	98.57(6)	N(6)–Ni(1)–N(4)	96.2(3)
Cl(2)–Pb(2)–I(3)	91.81(6)	N(6)–Ni(1)–N(2)	92.6(3)
I(5)–Pb(2)–I(3)	90.71(3)	N(4)–Ni(1)–N(2)	95.0(3)
Cl(2)–Pb(2)–I(4)	160.34(5)	N(6)–Ni(1)–N(1)	91.1(3)
I(5)–Pb(2)–I(4)	100.95(3)	N(4)–Ni(1)–N(1)	171.2(3)
I(3)–Pb(2)–I(4)	90.24(2)	N(2)–Ni(1)–N(1)	79.7(3)
Cl(2)–Pb(2)–I(6)	85.31(6)	N(6)–Ni(1)–N(5)	78.5(3)
I(5)–Pb(2)–I(6)	103.25(3)	N(4)–Ni(1)–N(5)	89.4(3)
I(3)–Pb(2)–I(6)	166.00(2)	N(2)–Ni(1)–N(5)	170.5(3)
I(4)–Pb(2)–I(6)	88.00(2)	N(1)–Ni(1)–N(5)	96.9(3)
Cl(2)–Pb(2)–I(2)	80.55(6)	N(6)–Ni(1)–N(3)	171.9(3)
I(5)–Pb(2)–I(2)	172.97(2)	N(4)–Ni(1)–N(3)	78.9(3)
I(3)–Pb(2)–I(2)	82.36(3)	N(2)–Ni(1)–N(3)	94.2(3)
I(4)–Pb(2)–I(2)	80.36(3)	N(1)–Ni(1)–N(3)	94.4(3)
I(6)–Pb(2)–I(2)	83.65(3)	N(5)–Ni(1)–N(3)	95.0(3)

Symmetry transformations used to generate equivalent atoms: #1 $-x+1$, y, $-z+5/2$; #2 $-x+1/2$, $-y+3/2$, $-z+2$.

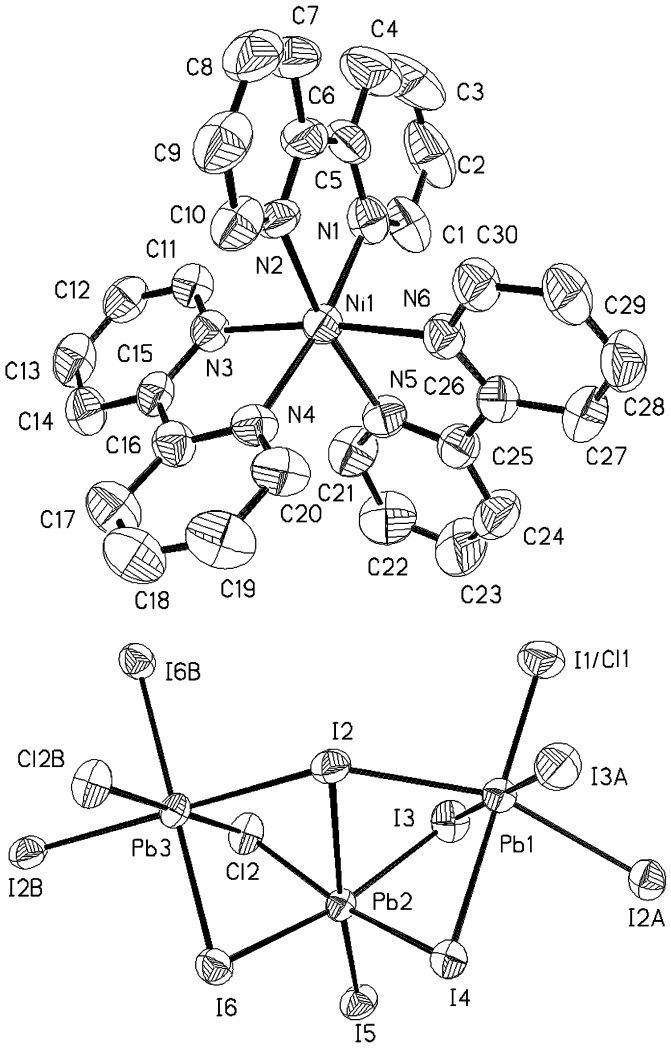

Fig. 1. Ellipsoid plots of the cation (top) and anion (down) of compound **1** (without DMF molecule) showing the atom labeling scheme. Displacement ellipsoids are drawn at the 50% probability level and H atoms have been omitted for clarity. [Symmetry code: (A) $-x+1$, y, $-z+5/2$; (B) $-x+1/2$, $-y+3/2$, $-z+2$.]

other NiX_2 (X = F or Br) in place of $NiCl_2$ under the same condition have also been carried out to prepare fluoride/iodide or bromide/iodide of lead, but unfortunately, no crystal was suitable for X-ray single-crystal analysis. In general, syntheses of the compounds are not only closely related to the geometry and the number of coordination sites provided by metal ions or ligands, but also controlled by the environment conditions (such as: reactants, metal-to-ligand ratio, countercations, solvents, temperature, pH value, etc.). Thus, this preparation may mainly depend on the choices of both reactants and the PbI_2/NaI/$NiCl_2$ stoichiometry.

3.2. Structure description

The title compound $[Ni(bipy)_3Pb_2I_{4.84}Cl_{1.16}\cdot DMF]_n$ (**1**) is composed of polymeric $[Pb_2I_{4.84}Cl_{1.16}]_n^{2n-}$ mixed haloanions, magnetic $[Ni(bipy)_3]^{2+}$ cations and DMF molecules (Fig. 1). In this compound, there are three crystallographically independent Pb atoms in slightly distorted $[PbX_6]$ octahedral coordination environment. Two $[Pb(3)X_6]$ octahedra and one $[Pb(2)X_6]$ octahedron connect through *trans* common faces (Cl(2)–I(2)–I(6)) to form a trimer, in which Pb(2) atom is on an inversion center; the adjacent trimers are joined by $[Pb(1)X_6]$ octahedron with *cis* common faces (I(2)–I(3)–I(4)) to form a wave-shape anion chain extending along [101] direction (Fig. 2). Such a one-dimensional mixed haloanion has, to the best of our knowledge, never been reported in the literature.

As a consequence of the connectivity of $[PbX_6]$ octahedra in compound **1**, the halo ligands are acting as μ_3 (I(2), I(4)) and μ bridges (Cl(2), I(3), I(6)) and as terminal ligands (I(5), I(1)). The terminal I(1) actually is halide mixing I(1)/Cl(1) with Pb(1)–I(1) bond length of 2.9479(17) Å. The Pb–μ-I and Pb–μ-Cl bond lengths are in

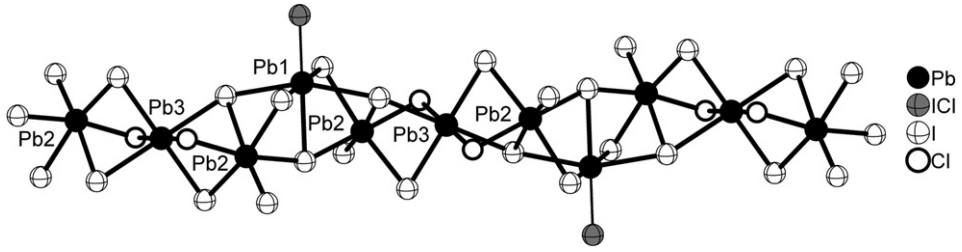

Fig. 2. Fragment of the $[Pb_2I_{4.84}Cl_{1.16}]_n^{2n-}$ anion in **1** extending along [101] direction.

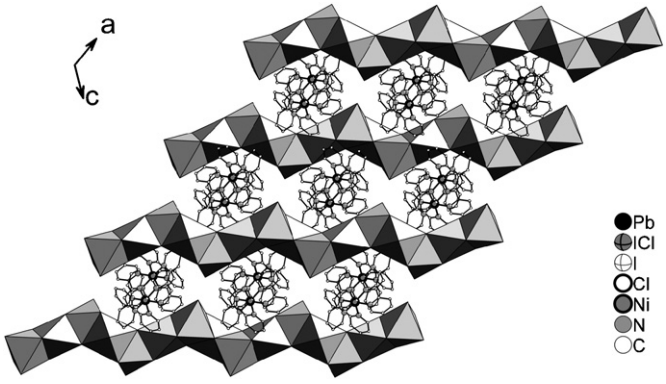

Fig. 3. Packing view of compound **1**. Pb polyhedra are shown in gray. The hydrogen atoms and DMF molecules are omitted for clarity.

Table 3
Hydrogen bond distances (Å) and angles (deg) for compound **1**

C–H···A	*d*(C–H)	*d*(H···A)	*d*(C–A)	∠ (CHA)
C(7)–H(7)···I(3)#1	0.93	3.06	3.863(17)	146
C(11)–H(11)···O(1)#2	0.93	2.59	3.182(17)	122
C(12)–H(12)···O(1)#2	0.93	2.52	3.143(19)	124
C(19)–H(19)···I(3)#3	0.93	3.03	3.950(12)	169
C(21)–H(21)···O(1)#4	0.93	2.42	3.204(19)	142
C(23)–H(23)···I(4)#5	0.93	3.03	3.805(17)	141
C(23)–H(23)···I(4)#6	0.93	3.03	3.805(17)	141

Symmetry transformations used to generate equivalent atoms: #1 $-x+1$, y, $-z+5/2$; #2 $x+1/2$, $y+1/2$, $z+1$; #3 $-x+1/2$, $-y+3/2$, $-z+2$; #4 $-x$, $-y+1$, $-z+1$; #5 $x-1/2$, $y+1/2$, z; #6 $-x+1/2$, $y+1/2$, $-z+5/2$.

the range of 3.1185(12)–3.2792(10) and 2.851(3)–2.860(2) Å, respectively, in accordance with corresponding lengths in chains of face-sharing $[PbX_6]$ octahedra [12]. The longest Pb–I bond length is observed for the triply bridging ligand I(2) (Pb(2)–I(2) 3.4705(9) Å) due to its higher connectivity and the *trans* influence of the terminal ligand I(5) (Pb(2)–I(5) 3.0232(9) Å) in *trans* position to I(2) [13].

The $[Pb_2I_{4.84}Cl_{1.16}]_n^{2n-}$ mixed haloanions are surrounded by $[Ni(bipy)]^{2+}$ cations and DMF molecules to form a crystal structure (Fig. 3). It should be pointed out that the six-coordinated nitrogen atoms of three bipy ligands form a distorted octahedron around discrete Ni atom. The Ni–N bond lengths have a range of 2.079(7)–2.094(7) Å; the two N atoms from each bipy ligand with the Ni atom form a five-membered chelate ring with the bond angle 78.5(3)–79.7(3)°. They compare well with that in compound $[Ni(bipy)_3][Pd(dmit)_2]\cdot CH_3CN$ with Ni–N = 2.064(3)–2.113 (3) Å and N–Ni–N = 78.2(1)−79.2(1)° [14]. The Ni···Ni distance is 8.3421(17) Å. Several cation–anion and DMF–anion hydrogen bonding interactions serve to direct the crystal packing; the details of these hydrogen bonding interactions are summarized in Table 3.

3.3. Diffuse reflectance spectroscopy

The optical band gap of **1** was assessed to be 2.59 eV by studying its diffuse reflectance spectroscopy (Fig. 4). The optical band gap is consistent with the yellow color of **1**, showing that the present compound belongs to semiconductor. According to the Kubelka–Munk function:

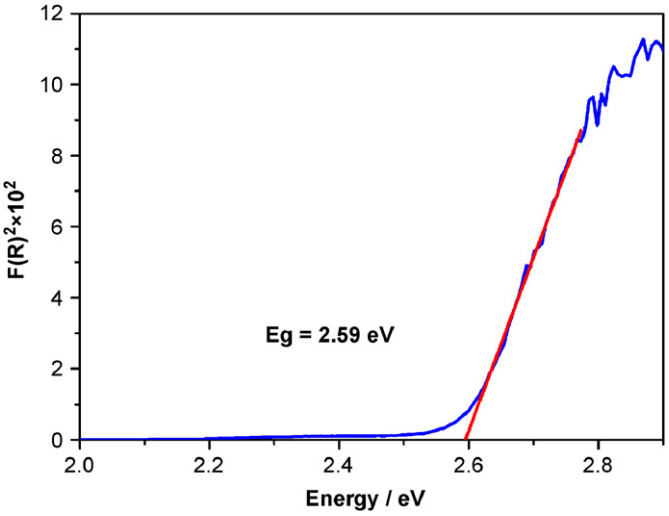

Fig. 4. Plot of $F(R)^2$ vs. photon energy for **1.**

$F(R) = (1-R)^2/2R$, in which R is the experimentally observed reflectance [15], the bandgap is determined as the intersection point of the energy axis with the extrapolated linear portion of the absorption edge in a $F(R)^2$ vs. photon energy plot.

3.4. Magnetic properties

The magnetic susceptibilities of **1** have been measured from ground crystals under a constant magnetic field of 5 kOe over the temperature range of 2–300 K. The data are

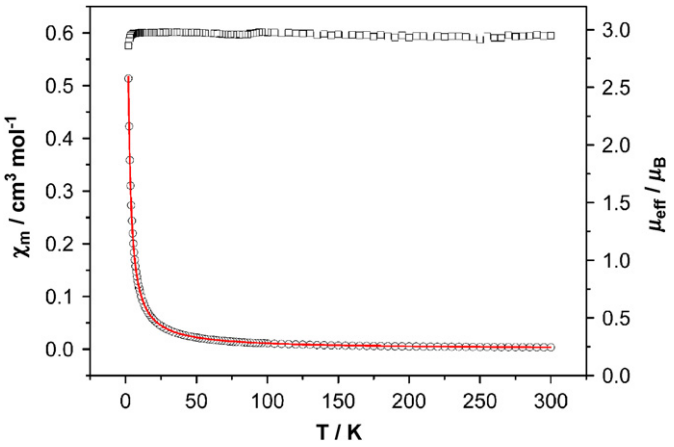

Fig. 5. Plots of μ_{eff} (□) and χ_m (○) vs. T over the temperature of 2–300 K at a field of 5 kOe, and theoretical fit (—) of χ_m data of **1**.

presented as plots of effective magnetic moment per mol μ_{eff} vs. T and molar magnetic susceptibility χ_m vs. T in Fig. 5. μ_{eff} basically stays at 2.96 μ_B in most temperature ranges, compared with the 2.83 μ_B expected for the noninteraction spin-only $S_{Ni} = 1$ ion, indicating the paramagnetic properties.

The magnetic data of **1** were analyzed in terms of a model of single-ion zero-field splitting (ZFS). First, after taking into account the Zeeman perturbation and ZFS, a magnetic susceptibility equation can be obtained as follows [9]:

$$\chi_{Ni} = (\chi_z + 2\chi_x)/3, \quad (1)$$

$$\chi_z = \frac{2Ng_z^2\beta^2}{kT}\frac{\exp(-D/kT)}{1+2\exp(-D/kT)},$$

$$\chi_x = \frac{2Ng_x^2\beta^2}{D}\frac{1-\exp(-D/kT)}{1+2\exp(-D/kT)},$$

where χ_{Ni} is the magnetic susceptibility in the absence of an exchange field and D is the ZFS parameter. Second, because of the weak dipole interactions, expression (1) may be corrected based on the molecular field approximation, which is illustrated in Eq. (2),

$$\chi_{Ni} = \frac{\chi_{Ni}}{1 - 2zJ\chi_{Ni}/Ng^2\beta^2}, \quad (2)$$

where χ_{Ni} is the magnetic susceptibility actually measured, zJ is the exchange parameter for dipole interactions, and the rest of the parameters have their usual meanings. Fitting to Eq. (2) gives a set of the best-fitting parameters with $D = 0.42\,cm^{-1}$, $g = 2.12$, and $zJ = 0\,cm^{-1}$. An agreement factor defined as $R = \sum(\chi_m^{obs} - \chi_m^{cal})^2/\sum(\chi_m^{obs})^2$ is 4.86×10^{-7}. The zJ value, which is the exchange parameter for dipole interactions, also suggests that paramagnetic properties exist in **1** again.

3.5. Thermal stability

To study the stability of this material, thermogravimetric analysis (TGA) was performed on polycrystalline sample of this compound (see Fig. 1 of the Supplementary Materials). TGA revealed that the first weight loss in **1** started at ca. 142 °C up to 166 °C to give a weight loss of ca. 4.43%, corresponding to the loss of one DMF molecule per formula unit (4.38% calculated). On further heating, it lost three bipy ligand molecules between ca. 240 and 482 °C (ca. 29.13% observed, 28.01% calculated). In the following weight loss, this compound continued to decompose gradually, and the resulting black unknown residue was found after complete decomposition.

4. Conclusions

While a number of haloplumbates materials have been synthesized and structurally characterized, materials containing mixed haloanions of lead are comparatively rare. Herein, we have described a facile approach for the preparation of such materials. And magnetic complex has been used to tune the structure of mixed haloanion of haloplumbate to form magnetic semiconductor exhibiting the magnetic and semiconducting properties simultaneously. Current synthetic efforts are directed at the preparation of mixed-metal haloplumbate material; as such materials may also exhibit interesting magnetic, optical, electronic properties. Further studies are in progress in our laboratory.

Acknowledgments

This work was supported financially by the National Natural Science Foundation of China (Grant nos. 50572030 and 50372022) and the Research Fund of Huaqiao University (Grant no. 06BS216).

Appendix A. Supplementary data

Supplementary data associated with this article can be found in the online version at doi:10.1016/j.jssc.2007.10.010.

Appendix A. Supplementary data

Listings of atomic coordinates and thermal parameters, and TG curve for **1** are provided as supplementary materials. Crystallographic data for the structure reported in this paper have been deposited with the Cambridge Crystallographic Data Centre as supplementary publication no. CCDC655991. Copies of the data can be obtained free of charge on application to CCDC, 12 Union Road, Cambridge CB2 1EZ, UK (fax: +44 1223 336-033; e-mail: deposit@ccdc.cam.ac.uk).

References

[1] (a) D.B. Mitzi, S. Wang, C.A. Field, C.A. Chess, A.M. Guloy, Science 267 (1995) 1473;
(b) D.B. Mitzi, C.A. Field, C.A.W.T.A. Harrison, A.M. Guloy, Nature 369 (1994) 467;
(c) J. Calabrese, M.L. Jones, R.L. Harlow, N. Herron, D.L. Thorn, Y. Wang, J. Am. Chem. Soc. 113 (1991) 2328;
(d) A.M. Guloy, Z.-J. Tang, P.B. Miranda, V.I. Srdanov, Adv. Mater. 13 (2001) 833;
(e) G.A. Mousdis, G.C. Papavassiliou, C.P. Raptopoulou, A. Terzis, J. Mater. Chem. 10 (2000) 515;
(f) L.-Q. Fan, Y.-Z. Huang, L.-M. Wu, L. Chen, J.-Q. Li, E. Ma, J. Solid State Chem. 179 (2006) 2361;
(g) L.-Q. Fan, L.-M. Wu, L. Chen, Inorg. Chem. 45 (2006) 3149.

[2] (a) H. Krautscheid, F. Vielsack, Angew. Chem. Int. Ed. Engl. 34 (1995) 2035;
(b) C.P. Raptopoulou, A. Terzis, G.A. Mousdis, G.C. Pavassiliou, Z. Naturforsch. B 57 (2002) 645;
(c) Z.-J. Tang, J. Guan, A.M. Guloy, J. Mater. Chem. 11 (2001) 479;
(d) H. Krautscheid, F. Vielsack, J. Chem. Soc. Dalton Trans. (1999) 2731.

[3] H. Krautscheid, F. Vielsack, Z. Anorg. Allg. Chem. 626 (2000) 3.

[4] (a) S.M. Wang, D.B. Mitzi, C.A. Feild, A.M. Guloy, J. Am. Chem. Soc. 117 (1995) 5297;
(b) X.H. Zhu, N. Mercier, M. Allain, P. Frère, P. Blanchard, J. Roncali, A. Riou, J. Solid State Chem. 177 (2004) 1067;
(c) Z.-J. Zhang, S.-C. Xiang, Y.-F. Zhang, A.-Q. Wu, L.-Z. Cai, G.-C. Guo, J.-S. Huang, Inorg. Chem. 45 (2006) 1972.

[5] (a) N. Mercier, Cryst. Eng. Commun. 7 (2005) 429;
(b) X.-H. Zhu, N. Mercier, A. Riou, P. Blanchard, P. Frère, Chem. Commun. (2002) 2160;
(c) X.-H. Zhu, N. Mercier, P. Fère, P. Blanchard, J. Roncali, M. Allain, C. Pasquier, A. Riou, Inorg. Chem. 42 (2003) 5330.

[6] A. Poglitsch, D. Weber, J. Chem. Phys. 87 (1987) 6373.

[7] T.M. Klapotke, B. Krumm, K. Polborn, C.M. Rienacker, Z. Naturforsch. B 55 (2000) 377.

[8] E. Coronado, P. Day, Chem. Rev. 104 (2004) 5419.

[9] O. Kahn, Molecular Magnetism, VCH, Weinheim, Germany, 1993.

[10] Rigaku, CrystalClear, version 1.3.6, Rigaku/MSC, Tokyo, Japan, 2005.

[11] G.M. Sheldrick, SHELXS97 and SHELXL 97, University of Göttingen, Germany, 1997.

[12] (a) H. Krautscheid, C. Lode, F. Vielsack, H. Vollmer, J. Chem. Soc. Dalton Trans. (2001) 1099;
(b) V.N. Kokozay, A.V. Sienkiewicz, Polyhedron 14 (1995) 1547;
(c) J.-W. Cai, J. Myrczek, I. Bernal, J. Chem. Soc. Dalton Trans. (1995) 611.

[13] (a) N.W. Alcock, Adv. Inorg. Chem. Radiochem. 15 (1972) 1;
(b) N.C. Norman, Phosphorus Sulfur Silicon Relat. Elem. 87 (1994) 167.

[14] M.J.J. Mulder, C. Faulmann, J.G. Haasnoot, J. Reedijk, J. Solid State Chem. 168 (2002) 390.

[15] G. Cao, L.K. Rabenberg, C.M. Nunn, T.E. Mallouk, Chem. Mater. 3 (1991) 149.